AJP

ISSN : 0971 - 3093

Vol 25, No 4 & 5, April and May, 2016

ASIAN JOURNAL OF PHYSICS

An International Quarterly Research Journal

ANITA PUBLICATIONS

FF-43, 1st Floor, Mangal Bazar, Laxmi Nagar, Delhi-110 092, India

B O : 2, Pasha Court, Williamsville, New York-14221-1776, USA

ap

Asian Journal of Physics
Vol. 25, No 4 & 5 (2016) 501-510
Available on: www.asianjournalofphysics.in

Resolution enhancement in digital holographic microscopy and tomography system

Balasubramani Vinoth, Yu-Chih Lin, Xin-Ji Lai, and Chau-Jern Cheng*
Institute of Electro-Optical Science and Technology,
National Taiwan Normal University, Taipei 11677, Taiwan

Dedicated to Prof FTS Yu

In digital holographic microscopy (DHM) achieving phase sensitivity is significant, which plays a major role in deciding the accuracy of the system. Our study elucidates the achievement of axial sub-nanometer precision with improvement in net phase sensitivity by instantaneous use of phase reference and temporal averaging techniques in DHM. To enhance the spatial resolution we implemented a synthetic aperture (SA) DHM system. The use of spectrum normalization method in SA-DHM system has helped to increase the spatial resolution and the phase sensitivity of the system. We also demonstrated the 3D imaging method based on sectional imaging technique to measure the refractive index variation between the spliced end of single mode fiber and the polarization maintaining fiber with digital holographic microscopy and tomography system (DHMT).

Keywords: Digital holographic microscopy (DHM), Spatial resolution, Phase sensitivity, Tomography system.

1 Introduction

Digital holography (DH) [1] is an imaging method based on interference principle, in which the object wave is superimposed with the reference wave and the output image is recorded as a hologram, a numerical reconstruction algorithm [2] is used to reconstruct the object information. Holography system consists of a laser source, interferometer and a camera to capture the hologram. In general, the interferometer configurations used are Michelson or Mach-Zehnder interferometer but the most commonly used method is Mach-Zehnder interferometer configuration. Then DH evolved a new era in imaging method by introducing microscope objective into its optical path and the system is renamed as digital holographic microscopy (DHM) system with numerous applications [4-5]. In DHM system, obtaining a high phase sensitivity is more important to achieve a high precision system [6-7]. There are many proposed reconstruction methods [2-3] but only few studies are done to quantify the quality and phase accuracy towards the reconstructed images. Recent study [8-10] shows that the maximum phase accuracy can be achieved by eliminating the shot-noise effect induced by the image sensor. In this study we have improved the net phase accuracy of the DHM system by using spatial and temporal averaging technique. Then a synthetic aperture digital holographic microscopy (SA-DHM) is developed to enhance the spatial resolution of the system. SA-DHM system records consecutive holograms at different incident angles and the holograms are synthesized to produce a high quality image of the object [11-12] . This method will enhance the lateral and axial resolutions of the system [13-14]. Digital holographic microscopy is a highly effective method [13-16] especially in the field of topography and morphology measurements of transparent or reflective objects such as micro-optical elements, micro-electromechanical (MEMS) devices, and biological cells [17]. The recent trend in DH is to develop a high quality tomographic imaging system [18]. This tomography system can provide a quantitative phase measurements, in which the refractive index and thickness of the sample can be assessed [19]. There

Corresponding author :
e-mail:cjcheng@ntnu.edu.tw (Chau-Jern Cheng)

are several proposed tomographic imaging methods exists based on DH but there are two common optical configuration are followed which is either by sample rotation [20] or by beam rotation method [21]. It is hard to follow the sample rotation type method for any liquid or biological specimen as it would get disturbed while rotating. So we also developed a novel experimental architecture to study the refractive index distribution inside the specimen.

This paper has various sections. In first it talks about the principle of digital holographic microscopy system, second part will describe the phase accuracy measurement in DHM system based on spatial and temporal averaging method. Third part will discuss about the enhancement of spatial resolution in synthetic aperture digital holographic microscopy system by spectrum normalization method. Final part will talk about the development of tomographic imaging system based on coaxial rotation method.

2 Digital holographic microscopy (DHM)

In conventional microscopy system the projected image of the object will be recorded directly, on the other hand digital holographic microscopy record it as a hologram and a numerical reconstruction algorithm leads to obtain a quantitative phase contrast image. The basic DHM setup consists of a coherent laser source, interferometer setup, digitizing (e.g. a CMOS or CCD) camera and a computational device. Typical interferometer used is Mach-Zehnder interferometer configuration. Optical layout of a conventional DHM experimental setup is shown in Fig 1.

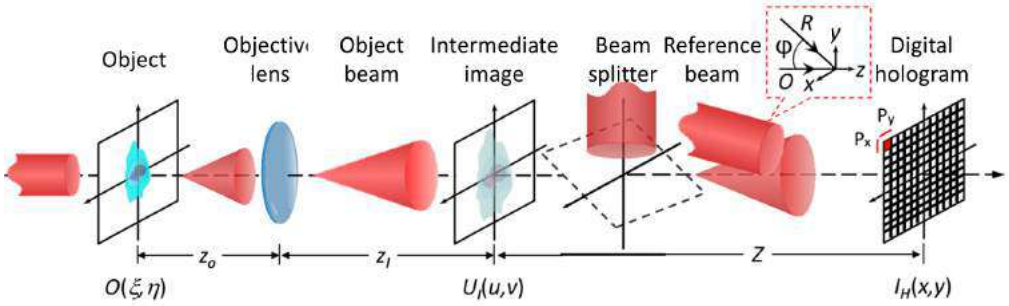

Fig 1. Schematic of digital holographic microscopy system.

The coherent laser beam is divided into object beam (O) and reference beam (R) by a beam splitter. Both O and R traces a different optical path but with a same propagation distance. The microscope objective is introduced in the object beam's path which produces a magnified image of the sample. Then the reference wave is superimposed with the object wave by a beam splitter with a considerable amount of tilt angle against the object wave to generate off-axis hologram which is recorded by a CCD camera. After recording, the reconstruction can be done either by experimentally or by computationally. There are several computational methods are available to reconstruct the recorded hologram but the most commonly used one is angular spectrum method (ASM) [2-3] because of its effective computation with highest degree in accuracy. The angular spectrum method is expressed as,

$$U(x,y;z) = \int\int U(k_x,k_y;z)\exp[i(k_x x + k_y y)]\mathrm{d}k_x,\mathrm{d}k_y$$
$$= F^{-1}\{\mathrm{filter}[F\{U_i\}]\exp[i\,k_z z]\} \quad (2.1)$$

where U_i is the complex object information.

The angular spectrum $U(k_x, k_y; z)$ is expressed as,

$$U(k_x, k_y; z) = \tilde{U}(k_x, k_y; 0)\exp[i\,k_z z] \quad (2.2)$$

where U_i is the complex object information, $\tilde{U}(k_x, k_y; 0)$ is angular spectrum at $z = 0$ and $k_z = \sqrt{(k^2 - k_x^2 - k_y^2)}$ where k_x and k_y are corresponding spatial frequencies along x and y axis, respectively.

ASM is used to eliminate the zero order and twin image disturbance, which also eliminates the minimum distance requirement along z-axis. With this algorithm the next section will elaborate the techniques for the accurate phase measurement in DHM system.

3 Phase measurement accuracy in DHM

3.1 Experimental Description

The schematic of the phase measurement setup in digital holographic microscopy system is shown in Fig 2(a). The laser diode with a center wavelength of 659 nm is used and it can be operated either in single or multi-mode by combining a reflective volume holographic grating (VHG) [15] and a current-driven temperature controller (CTC). It has a spectral bandwidth of 0.07 nm at single mode and 0.68 nm at multimode operation with an output power of 35 mW. By switching from single mode to multi-mode within a source will avoid the disturbances in spatial intensity distribution, optical alignment mismatch and also the optical beam traces the same path for both the configurations. The spectral response of a single mode (Fig 1.b) and a multi-mode (Fig 1.c) operation is shown.

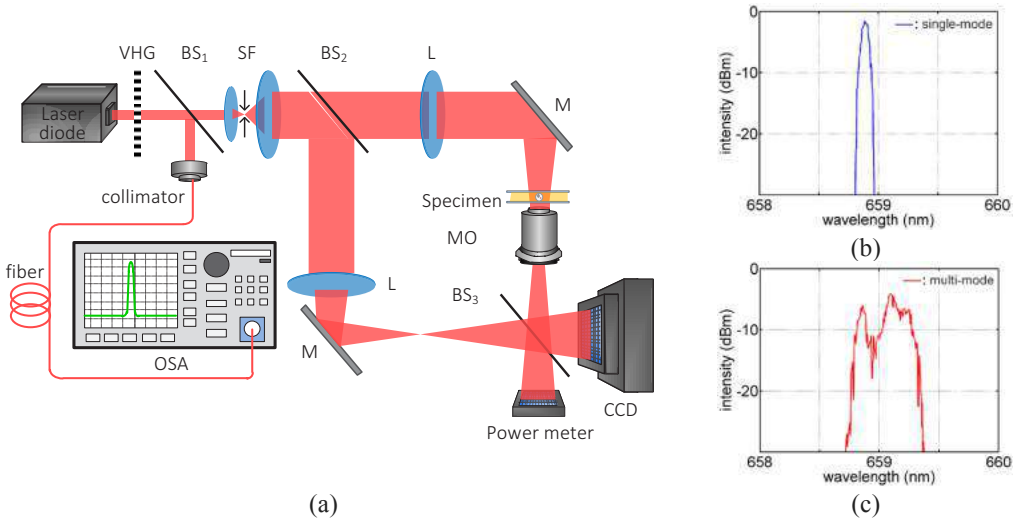

Fig 2. (a) Schematic of phase measurement setup of digital holographic microscopy using a wavelength-stabilized laser operated in (b) single-mode and (c) multi-mode.

The laser beam is split into two by beam splitter (BS_1), a part of the beam is coupled into a fiber collimator and the spectral behavior is recorded by using optical spectrum analyzer (OSA) (Anritsu MS9710C). The spectral resolution of the OSA was limited to 0.07 nm. The CTC is adjusted in order to choose the operation mode of the laser diode in a DHM system for the coherent illumination. The other part of the beam BS_1 is used as the input to the off-axis Mach-Zehnder interferometer configuration. In the object arm a microscope objective with a magnification of 40× is used to magnify the specimen. An angled reference wave is superimposed with object wave at BS_3 to generate a hologram and the same is recorded by a CCD (1,392×1,040 pixel size, (6.45×6.45) μm^2 pixel pitch). To avoid shot noise domination a part of the optical beam from BS3 is monitored by a power meter which helps to maintain the constant number of photons (18,000 photons/pixel approx) falls on the CCD to obtain high phase accuracy [13].

3.2 Measurement method

To eliminate the phase fluctuations from CCD and Laser diode, several holograms $\{P_1, P_2 \ldots P_N\}$ are recorded without specimen. From the recorded holograms, an average is estimated and set this to be a phase reference (P_r) which will be subtracted from object hologram. This will effectively reduce the spatial fluctuation from the optical elements and the shot noise dominations from the CCD.

The resulting phase image after phase referencing is expressed as

$$P_{sa} = P_i - P_r,\ i = 2,3,\ \ldots,\ N \tag{3.1}$$

Now constant phase level is achieved but no correction in temporal phase fluctuations are involved. To correct the random fluctuations of the laser diode, temporal averaging technique is applied and can be expressed as:

$$P_{ta} = \frac{\sum_{i=1}^{N}(P_i - P_r)}{N=1},\ i = 2,3,\ \ldots,\ N \tag{3.2}$$

By applying phase referencing and temporal averaging technique, the net phase accuracy is improved and the axial resolution can be determined with the known refractive index and the wavelength of the source. For better understanding the axial accuracy is expressed in relation to the axial resolution of optical path length.

3.3 Results and Discussion

We have achieved a sub-nanometer level phase accuracy measurement system. The measurement results in Fig 3 indicate that the step height before phase referencing (measured about 86.5 nm ± 6.1 nm) and after phase referencing (measured about 84.4 nm ± 1.2 nm), the phase sensitivity of the system is increased. The efficient DHM system will not only focus on the phase accuracy but also the other two important parameters such as lateral and axial resolutions of the system to achieve a better quality image. The next section will discuss about the achievement of lateral and axial resolutions with super resolution synthetic aperture digital holographic microscopy system.

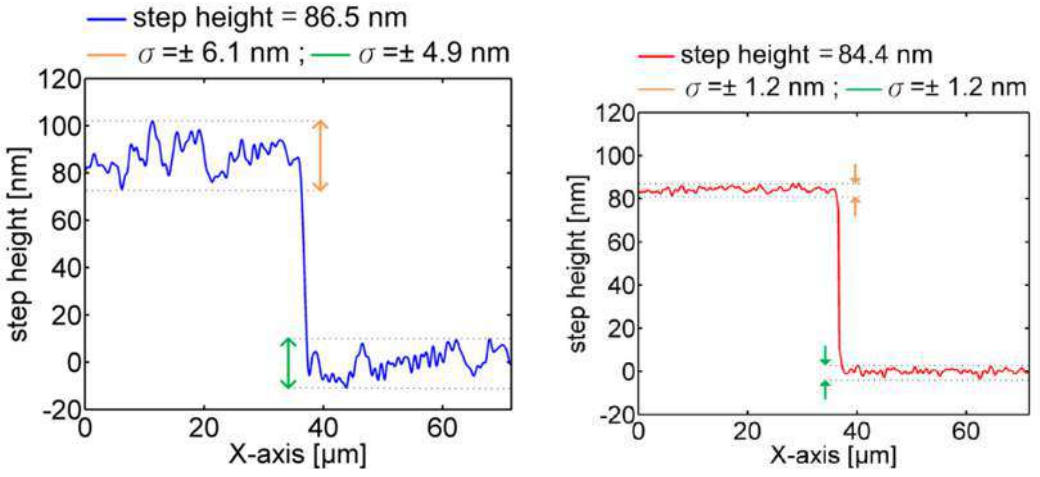

(a) (b)

Fig 3. Experimental results of calibrated step height standard (a) before phase referencing (b) after phase referencing technique.

4 Super resolution synthetic - aperture digital holographic microscopy system

4.1 Principle and experimental method

We modified the optical design and implemented a spectrum normalization method to achieve a super resolution with the synthetic aperture digital holographic microscopy (SA-DHM) system. The experimental set up consists of an extra component a galvo- mirror in the object arm to produce different incident angles on the specimen, then it will be superimposed with the reference wave to generate a hologram which will be recorded by CCD. The schematic of synthetic aperture digital holographic microscopy system is shown in Fig 4.

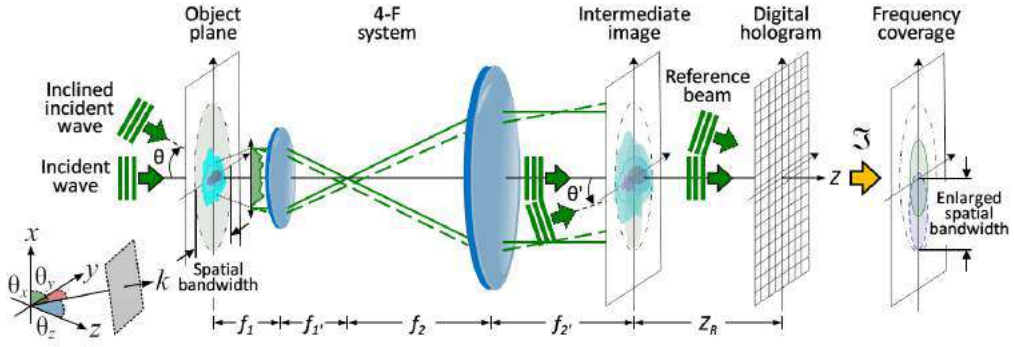

Fig 4. Schematic of synthetic aperture digital holographic system

First step in synthetic aperture technique is to record the hologram at different incident angles. Fourier transform of the recorded holograms will yield the different frequency bands and the complete frequency coverage for image reconstruction is increased by integrating those different frequency bands. The overall synthesized spectrum after SA is expressed as:

$$U_{SA} = \sum_{m=1}^{M} \sum_{n=1}^{N} A(u,v) e^{j\phi(u,v)} \cdot \left[\mathrm{H}(u,v) \oplus \delta\left(u + \frac{a_m}{\lambda}, v + \frac{\beta_n}{\lambda} \right) \right] \tag{4.1}$$

The spatial frequency band is represented as a circular aperture function, $\mathrm{H}(u,v) = \mathrm{circ}(\sqrt{u^2 + v^2}/f_0)$, f_0 is the cutoff frequency at normal incidence, m and n are the number of frequencies to be synthesized, M and N are the number of exposures for the hologram recording. To perform spectrum normalization, an inverse apodization window function is created and applied to reduce the excessive frequency overlapping along the scanning direction.

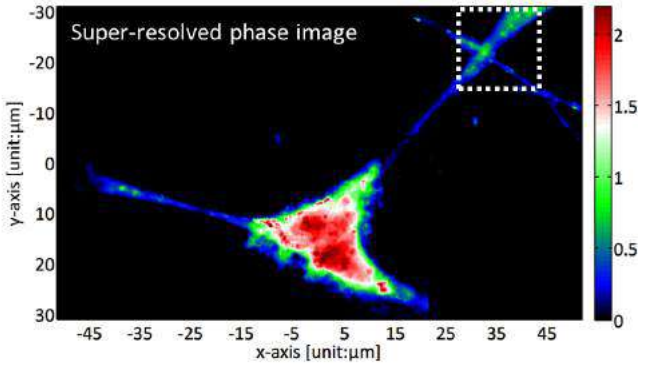

(a)

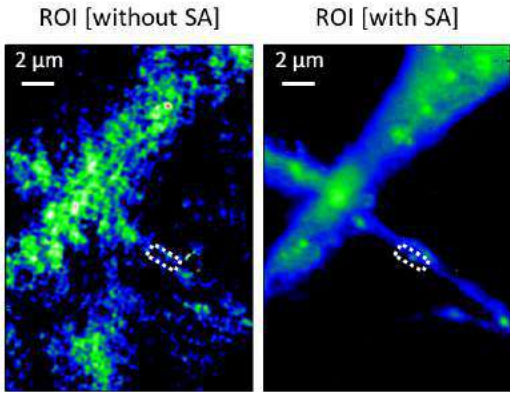

(b)

Fig 5. Experimental results of SH-SY5Y living cell (a) wide-filed super-resolved phase image and (b) ROI of neurite before and after SA.

4.2. Results and Discussion

We have extended the lateral and axial resolutions of the system with super resolution synthetic aperture digital holographic microscopy (SA-DHM) system. Using a coherent light system, the ideal experimental resolution for this system is 0.4 µm, whereas this is increased by twice using the super resolution SA-DHM system which is about 0.2 µm. The phase variations is approximately measured as 0.13 rad (for hologram $N = 450$) and 0.15 rad (for hologram $N = 35$). The experimental results showed that the synthetic spectrum normalization method could substantially reach high phase sensitivity using only a few numbers of holograms ($N = 35$). Figure 5 shows the wide-field capability of SA-DHM with motorized x-y stage and the organelle in neurite can be clearly observed after synthetic aperture. With modification in optical design SA-DHM system, a tomographic imaging system is developed to generate the three dimensional (3D) image of the specimen. The next section has analyzed more in detail to generate the 3D image of the specimen.

5 Tomographic imaging using digital holographic microscopy system

Tomographic method is used to generate a three dimensional (3D) image of the specimen. In general, there are two common methods that are followed to generate the 3D image of the specimen. First one is by beam rotation method, the optical set up is quite same as shown in the Fig 6 which has a Mach–Zehnder interferometer with a galvo-mirror in the object arm and a CMOS sensor is used to record the hologram. The galvo- mirror will steer the optical beam at different incident angles. The drawback of the beam rotation method is that the system resolution is limited by the numerical aperture of objective lens used but the specimen will remain undisturbed. Second one is by specimen rotation method, there is no limitation here as like in the beam rotation method, here the specimen can even rotate at 360° to get the complete 3D information of it but there might be a chance where the specimen can gets disturbed.

5.1 Tomographic imaging by coaxial rotation method

5.1.1 Principle and experimental method

By considering the merits of beam rotation method and by implementing few changes in optical configuration we developed a new experimental approach based on beam rotation method to acquire entire 3D information of the specimen and this method is known as coaxial rotation method. The diagrammatic explanation of the coaxial rotation method is shown in Fig 6. The incident beam and the CCD sensor are lined up linearly and it can be rotated around the specimen simultaneously. Consider the refractive index of the

specimen and the surrounding medium as n_s and n_m, respectively. The spatial resolution of the reconstructed image is explained in Ref [19]. The maximum lateral and axial resolutions is related with the wave vector (k), incident angle (θ_i) and the numerical aperture (NA) of the objective used.

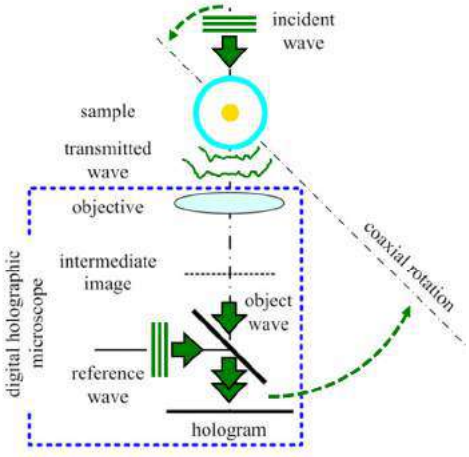

(a)

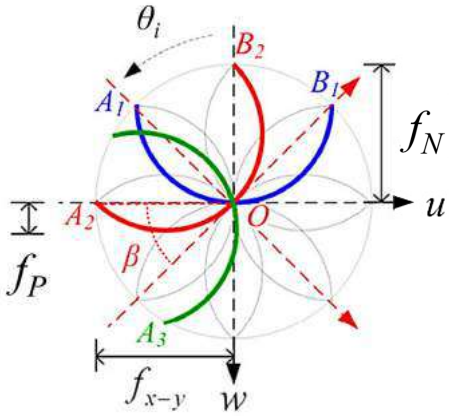

(b)

Fig 6. (a) Working principle of coaxial rotation digital holographic microscopy and tomography method and (b) frequency distribution in 2D

The complete axial cutoff frequency coverage in both positive (f_P) and the negative ($f_{N)}$ directions is expressed as:

$$f_P = \begin{cases} k\,NA\left(\dfrac{\sin(\theta_i-\beta)}{\cos\beta} + 1 - \sqrt{\cos^2\theta_i} + \dfrac{2}{\cos\beta}\sin(\theta_x-\beta)\cos\theta_i + \dfrac{\sin^2\theta_i}{\cos^2\beta}\right) \\ \dfrac{k\,NA}{\cos\beta}\sin(\theta_i-\beta), \qquad \text{for } 90° \le \theta_i \le (\beta+90°) \end{cases} \tag{5.1}$$

$$f_N = \frac{k\,NA}{\cos\beta}\sin(\theta_i-\beta) \tag{5.2}$$

From Fig 6 (b), it is clear that the rotation angle is directly proportional to the axial and lateral resolutions of the system. The schematic of the coaxial rotation digital holographic microscopy and tomography experimental setup is shown in Fig 7.

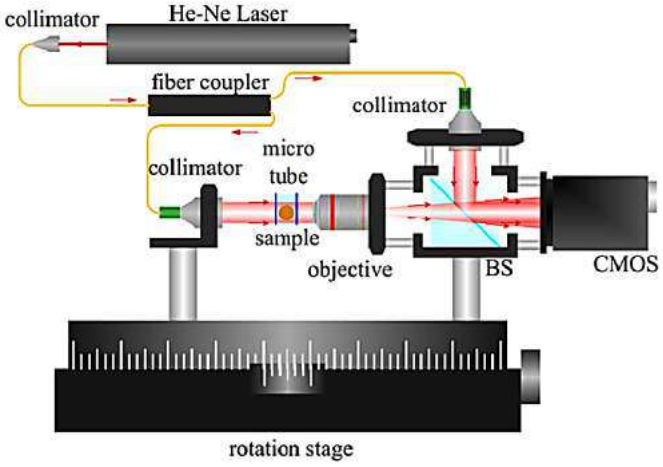

Fig 7. Schematic of coaxial rotation digital holographic microscopy and tomography system

The experimental system consists of He-Ne laser source (632.8 nm), fiber coupler, Mach-Zehnder interferometer (MZI) and a CMOS camera which has (1,280×1,024) pixels with a pitch of (5.2×5.2) μm^2. The laser source is split into two by a fiber coupler, a part of the beam is passed through the fixed specimen container and it is superimposed with the other part of the beam. The corresponding hologram is recorded by a CMOS camera. The complete interferometer setup is mounted on a motorized rotational stage to generate a hologram information of the specimen at a different incident angles varying from 0° to 360° with 1° step angle variation. Enough settling time (1 sec) between each degree is programmed to the rotational stage to avoid the mechanical vibrations during the hologram recording.

5.1.2 Results and discussions

By using this method, we tried to measure the refractive index distribution between the single mode (Corning HI 1060) fiber which has approximately 1.464 refractive index with 5 μm core diameter and the polarizing maintaining (Corning PANDA PM1550) fiber. Figure 8(a) shows the *x-y* sectional image of the joint in the fused fiber, which is marked as a red dashed line. The refractive index distribution before the fused end is shown in Fig 8(b) which corresponds to single mode fiber. The refractive index distribution close to the fused end is shown in Fig 8(c) and the refractive index distribution after the fused end is shown in Fig 8(d), which corresponds to polarization maintaining fiber and also the panda like structure is observed clearly.

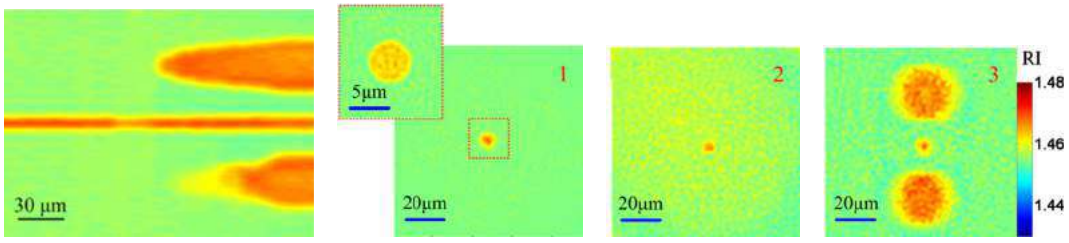

Fig 8. Experimental results of the fused fiber structure (a) *x-y* sectional image, and *x-z* sectional images at (b) point 1, (c) point 2, and (d) point 3, of the spatially refractive index distribution inside the fused fiber.

6 Conclusions

A sub-nanometer level phase accuracy is achieved by implementing the spatial reference and temporal averaging method in digital holographic microscopy system. The spatial resolution and phase sensitivity of the system is enhanced by using spectral normalization method for strengthening the high frequency information. The experimental results showed that the synthetic aperture spectrum normalization method can substantially reach high phase sensitivity using only a few numbers of holograms. A sample rotational experimental setup is developed to generate a 3D image by coaxial rotation method. The spatial refractive index distribution inside the fiber is analyzed with digital holographic microscopy and tomography system based on coaxial rotation method. This technique can be used to generate a high quality 3D image of a biological tissues by replacing the existing objective into another objective with high numerical aperture.

Acknowledgment

This work was financially supported in part by the Ministry of Science and Technology (MOST), Taiwan.

References

1. Poon T C, Digital Holography and Three-Dimensional display: Principles and Applications, (Springer, New York), 2006.
2. Kim M K, Digital holographic Microscopy; Principles, Techniques and Applications, (Springer, New York), 2011.
3. Goodman J W, Introduction to Fourier optics, (Roberts & Co, Greenwood), 2004.
4. Liu C, Liu Z G, Bo F, Wang Y, Zhu J Q, Super resolution digital holographic imaging method, *Appl Phys Lett*, 81(2002)3143-3145.
5. Micó V, Zalevsky Z, Martínez P G, García J, Synthetic aperture superresolution with multiple off-axis holograms, *J Opt Soc Am A*, 23(2006)3162-3170.
6. Massig J H, Digital off-axis holography with a synthetic aperture, *Opt Lett*, 27(2002)2179-2181.
7. Kozacki T, Krajewski R, Kujawi´nska M, Reconstruction of refractive-index distribution in off-axis digital holography optical diffraction tomographic system, *Opt Express*, 17(2009)13758-13767.
8. Charriere F, Rappaz B, Kuhn J, Colomb T, Marquet P, Depeursinge C, Influence of shot noise on phase measurement accuracy in digital holographic microscopy, *Opt Express*, 15(2007)8818-8831.
9. Colomb T, Kuhn J, Charriere F, Depeursinge C, Marquet P, Aspert N, Total aberrations compensation in digital holographic microscopy with a reference conjugated hologram, *Opt Express*, 14(2006)4300-4306.
10. Cotte Y, Toy M F, Depeursinge C, Beyond the lateral resolution limit by phase imaging, *J Biomed Opt*, 16(2011)106007; doi:10.1117/1.3640812
11. Bühl J, Babovsky H, Kiessling A, Kowarschik R, Digital synthesis of multiple off-axis holograms with overlapping Fourier spectra, *Opt Commun*, 283(2010)3631-3638.
12. Lai X J, Tu H Y, Wu C H, Lin Y C, Cheng C J, Resolution enhancement of spectrum normalization in synthetic aperture digital holographic microscopy, *Appl Opt*, 54(2015)A51-A58.
13. Hillman T R, Gutzler T, Alexandrov S A, Sampson D D, High-resolution, wide-field object reconstruction with synthetic aperture Fourier holographic optical microscopy, *Opt Express*, 17(2009)7873-7892.
14. Lee Y L, Lin Y C, Tu H Y, and Cheng C J, Phase measurement accuracy in digital holographic microscopy using a wavelength-stabilized laser diode, *J Opt*, 15(2013)025403; oi.org/10.1088/2040-8978/15/2/025403
15. Kim M, Choi Y, Yen C F, Sung Y, Dasari R R, Feld M S, Choi W, High-speed synthetic aperture microscopy for live cell imaging, *Opt Lett*, 36(2011)148-150.
16. Choi Y, Kim M, Yoon C, Yang T D, Lee K J, Choi W, Synthetic aperture microscopy for high resolution imaging through a turbid medium, *Opt Lett*, 36(2011)4263-4265.

17. Lin Y C, Cheng C J, Determining refractive index profile of micro-optical elements using ransflective digital holographic microscopy, *J Opt*, 12(2010)115402; doi.org/10.1088/2040-8978/12/11/115402
18. Cheng C J, Lai X J, Lin Y C, Image formation of digital holographic microtomography OSA Topical Meeting on Digital Holography and Three-Dimensional Imaging, (Miami, USA, 2012) (Optical Society of America, 2012) paper DSu3C
19. Lin Y C, Cheng C J, Sectional imaging of spatially refractive index distribution using coaxial rotation digital holographic microtomography, *J Opt*, 16(2014)065401; doi.org/10.1088/2040-8978/16/6/065401
20. Kou S S, Sheppard C J R, Image formation in holographic tomography: high-aperture imaging conditions, *Appl Opt*, 48 (2009)H168-75.
21. Fauver M, Seibel E, Rahn J R, Meyer M, Patten F, Neumann T, Nelson A, Three-dimensional imaging of single isolated cell nuclei using optical projection tomography, *Opt Express*, 11(2005)4210-23.
22. Lee Y L, Lin Y C, Tu H Y, Cheng C J, Phase measurement accuracy in digital holographic microscopy using a wavelength-stabilized laser diode, *J Opt*, 15(2013) 025403; doi.org/10.1088/2040-8978/15/2/025403

[*Received*: 29.2.2016]